DOI:10.5937/jaes0-33912
Paper number: 20(2022)3, 992, 861-869
*www.engineeringscience.rs * ISSN 1451-4117 * Vol.20, No 3, 2022*

ANALYSIS OF VIBRATION SIGNATURE IN DEEP GROOVE BALL BEARING USING FINITE ELEMENT METHOD

Laxmikant G Keni, Padmaraj N H, Najiullah Khan, Jagadeesha P E, Pradeep R, Chethan K N*

Deptartment of Aeronautical & Automobile Engineering, Manipal Institute of Technology, Manipal Academy of Higher Education, Manipal, Karnataka, India
**chethanknarayan@gmail.com*

The most common kind of bearing is the rolling element bearing, which is a used mechanical component in rotating equipment that is subjected to heavy loads and rapid rotation. Bearing failure is the main consideration in the failure of rotating hardware. A deformity at any component of the bearing transmits to every single other component, for example, external race, inward race, ball, and retainer of the bearing. The simplest way to think about ball bearing failure examination is to create counterfeit cracks of varying sizes on various components of CATIA V-6 and write down their signatures. For this reason, the vibration investigation procedure which is dependable and precisely recognizing deformity in the bearing components is utilized. Estimation of the amplitude of vibrations is carried out at 5000 RPM, a load of 200 N, and at different deformity sizes, 3 mm and 4 mm on bearing races are carried out. A preparatory vibration investigation of a rolling component is carried out using Ansys R-18.0. Vibration signals for two diverse imperfection sizes have been extricated and a file for correlation of various deformity sizes has been proposed. The impacts of radial load, rotation speed, and starting deformity size on the stress level are studied.

Keywords:ball bearing, finite element method, vibration analysis, deformation, bearing failure

1 INTRODUCTION

A ball bearing is a kind of rolling-element bearing that makes use of balls to maintain the separation between the bearing races. A ball bearing's function is to minimize rotational friction and to sustain radial and axial loads [1][2]. This is accomplished via the use of at least three races to confine the balls and transfer the loads through them. The significance of early failure detection is addressed.

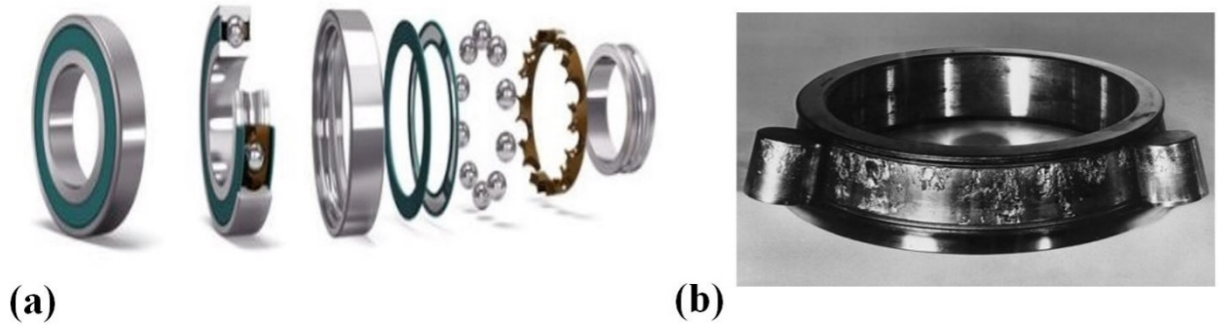

Figure 1: (a) Exploded view of bearing (b) Assembled bearing[3][4].

Figure 1 shows the exploded and assembled view of the bearing. Rolling element bearings are an imperative piece of all types of hardware[5]. Due to their far-reaching use and significance, their failure is regularly the reason for apparatus breakdown[6]. When a moving component's deformity makes contact with the surface of another component, an impact force is generated, causing the bearing to impulsively respond [7]. Any component deformity is transmitted to all other components, for example, the external &internal race, ball, and the bearing retainer.Subsequently, it is essential to screen the health of the bearing with the goal that the bearing can be supplanted before it fails[8].Deep groove ball bearings are used in pumps, gear boxes, motors, wind turbines etc. The important types of bearing problems are external outer race Internal inner race, defective balls, and cage. Cracks, pits, and spalls produced by rolling surface fatigue are examples of localized defects [9]. These defects may be the consequence of manufacturing errors or excessive abrasive wear. [10]. As a result, a study of the vibrations produced by these defects is critical for both quality assurance and condition monitoring.

Monitoring and analyzing vibration signatures is a critical method for predicting and diagnosing different defects in antifriction bearings. Vibration signature analysis offers early warnings of problems in progress and establishes the fundamental reference signature or baseline signature for future monitoring reasons. [11].

1.1 Bearing Defects

Thermal overloading of the bearing causes undesirable ripping off of the material, resulting in flaking of the surface. The setting, which frames on the bearing rings, is caused by a typical fatigue effect. This damage is the result of systematic stacking of bearing components and is caused by the material's normal fatigue. Small non-homogeneities in the material at a certain depth under the surface cause the first fractures.[12].Depressions and pressure damage to bearing rings are produced by the indelicate development of foreign particles in the raceway during bearing operation. In both instances, the degree of damage is excessive and may form the underlying site of dynamic fatigue harm – pitting. Abrasion occurs in the bearing as a result of ball glazing as a result of overloading and lubrication failures, as well as abrasion of the race as a result of spinning inside the seat [13].Both instances involve deplorable conditions. In addition to all the above-stated defects wear and corrosion is highly susceptible defects in ball bearing, When the moving surfaces of barrel-shaped rollers and races get worn due to a lack of lubrication without material chipping[14]. This kind of damage is more likely to occur in zones where the greasing-up film cannot be maintained. Corrosion takes place due to contact degradation on the raceway[15]. Degradation coming about because of deficient protection against dampness, or the utilization of an inadmissible lubricant is constantly impermissible.

1.2 Detecting the bearing defects

Bearing failure is a common cause of failures in rotating equipment, and a similar failure may be catastrophic, resulting in expensive downtime. One of the most critical aspects of bearing prognostics is detecting defects in their early stages and alerting the operator before they progress to catastrophic failure. The vibration analysis methodology is utilized to accomplish this since it is a very dependable and accurate method of identifying a fault in the bearing components.Rotating equipment is intricate and has many components that may fail. An examination should be performed to detect bearing problems before they cause catastrophic failure, resulting in substantial downtime costs and damage to other components of spinning equipment. Vibration spectrum analysis is a common method for monitoring equipment operating conditions, together with time-domain and time-frequency domain analysis [16]. This data can be collected through experimental and numerical approaches. Figure 2 illustrates an experimental test rig constructed to anticipate antifriction bearing defects. The shaft is driven by a variable-speed induction motor connected to a flexible coupling.[17]. To mitigate the impact of the motor's high-frequency vibration, the shaft is coupled using a flexible coupling.At the driver end, a self-aligning double-row ball bearing is installed, while the free end is equipped with a cylindrical roller bearing.The DC motor's control panel may provide a constantly changing speed.A tension rod is used to provide a radial load to the test bearing, which is then measured by a load cell. Between two support bearings is placeda test bearing. Split-type housings are ideal for installing and dismounting test bearings with ease. Before applying grease, bearings were thoroughly cleaned to remove any impurities.The vibration signals from both good and faulty bearings were monitored using a two-channel FFT analyzer. The FFT analyzer will be used to gather the vibration signatures for different operating parameters. We analyzed two distinct kinds of bearing defects: inner race and outer race. Analyses in the time domain and the frequency domain were conducted [11]

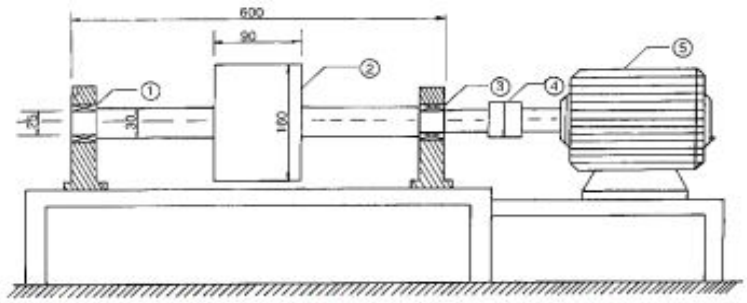

Figure2:-Schematic of test rig[11]

The magnitude of the defective bearing's spectrum at different harmonic frequencies is found to be very distinct in contrast to that of excellent bearings.For a fixed load, it is found that as the speed rises, the peak amplitude values steadily increase. Furthermore, the peak amplitude values for healthy bearings are lower than those for faulty bearings. The amplitude values for the outer race defect are found to be higher than those for the inner race defect. A flaw in the outer race causes the inner race to remain in the load zone at its maximum position, but in the second example, the inner race goes in and out of the load zone with each shaft revolution [18]. The finite element approach is one of the few techniques for taking care of entangled engineering issues. The finite element method's use is to solve complex problems by replacing them with simpler ones.Since the real problem is replaced by a simpler one when determining the arrangement, it may discover an inexact arrangement rather than the correct arrangement. Following that, the finite element method (FEM) is a methodology for numerical estimation.The fabrication of artificial defects of varying sizes on various parts and writing down their signatures are used to

investigate the failure analysis of ball bearings[6]. Artificial flaws are used in the bearing's finite element analysis to analyze the peaks at the outer and inner raceway defect frequencies. The amplitudes of vibration are thought to fluctuate with increasing speed at constant defect size and consistent load with varying rotation speeds. Similarly, for the same deformity measure, amplitudes of vibration are monitored greater for exterior ring bearings than for internal ring bearings.

2 MATERIALS AND METHODS

Modeling the bearing with a defect is carried out using CATIA V6. Parameters for the bearing specifications were defined so that they could be changed for any type of bearing that was to be analyzed. As a result, the parameters specified are the inner ring diameter, the diameter of the outer ring, the outer ring thickness, the raceway radius, the defect depth, the length, and the width.The modeling is carried in the assembly design section where the bearing was created with the dimensions of SKF bearing 6202 [19]. Figure 3 shows the SKF bearing 6202 used in the current study. Table 1 shows the dimensions considered during the modeling of the bearing.

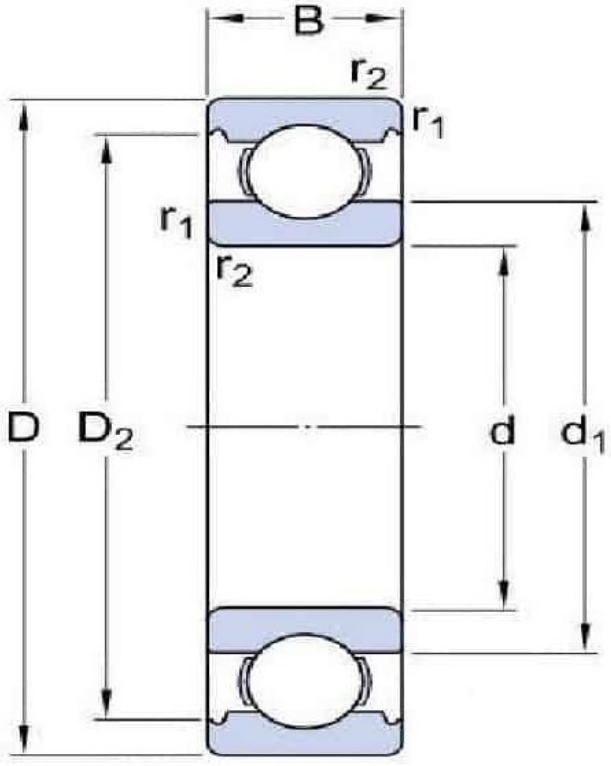

Figure 3:- Illustrated Dimensions of SKF Bearing 6202 [19].

Table 1**:** Dimensions of SKF Bearing 6202.

Dimension	Value(mm)
D	15
D	35
B	11
d1	21.7
D2	30.5
r1,2 min	0.6
Number of balls	7

Initially,the inner ring, outer ring, ball, and ball cage are modeled as per the geometrical dimensions given in table 1. A total of seven balls are modeled and the same in the ball cage the considered. All the models are assembled as shown in figure 4(a).

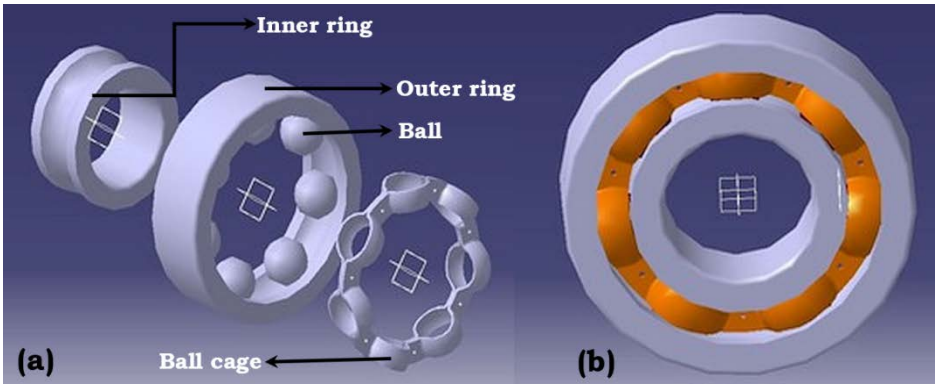

Figure 4: (a) separate components of bearing used in the analysis. (b) Assembled view of bearing.

2.1 Fault Generation

Two bearing models were modeled. Artificial faults to replicate real faults were generated by translation of the sketching plane to the plane of the race where the fault was to be created. Faults were created using such dimensions so that the bearing balls could fall out of place during operation to generate the required vibration signature[20]. Defects in the outer and inner rings were modeled by a cuboidal hole. The respective defects were created by translating a plane in the direction of the race, creating a square-shaped hole, and pocketing the aforementioned sketch to mimic the depth of the defect. 4mm fault was created on the inner race. A 5mm fault was created on the outer race. The flaws in the bearings' inner and outer races are shown in figure 5.

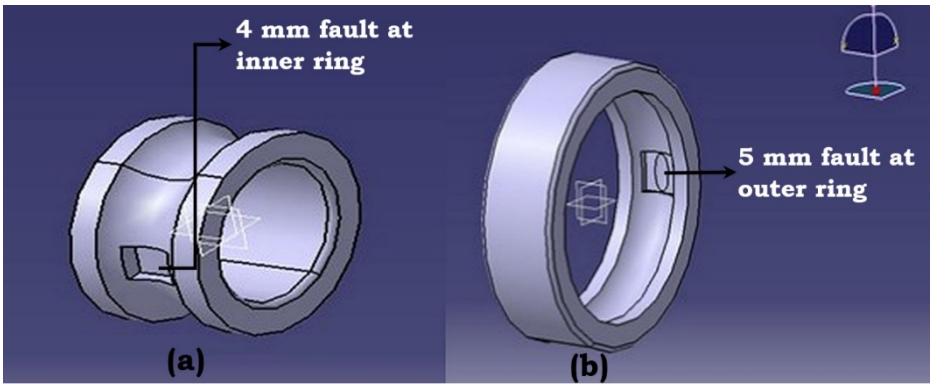

Figure 5: - (a) Defect in the bearing's inner ring (b) Defect in the bearing's outer ring.

The complete bearing is made of stainless steel, and the material characteristics are as shown in table 2. The material is considered linear isotropic.

Table 2:Mechanical properties of the stainless steel[21][22][23].

Properties	Value
TensileYieldStrength(MPa)	207
UltimateYield Strength(MPa)	586
Density(kg/m^3)	7750
Young'sModulus(MPa)	1.93E^{+05}
Poisson'sRatio	0.31
BulkModulus(MPa)	1.693E^{+05}

The contacts between the different parts of the bearings have to be defined. Ideally, the contact between the parts would be frictionless. But in practice, there will bea small amount of friction between the parts in contact. The dynamic coefficient of friction for a steel-steel type contact lies in the range of 0.4-0.6[22]. In the current work, the contact type is considered without lubrication.coefficient of frictionis considered to be 0.5 for all the analyses. The value of the friction/static coefficient is assumed to be equal to the dynamic coefficient.

2.2 Meshing

Unstructured mesh of mesh size 1mm is considered ensuing edge length is 0.36mm. the number of nodes and elements were 14704 and 36360 respectively. Figure 6 shows the completed meshed model and also the meshed model with the defect.

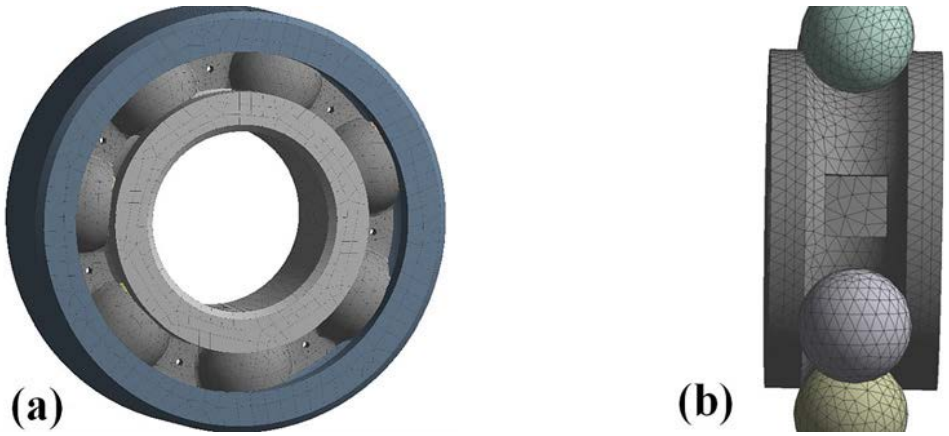

Figure 6: (a) Meshed model of the bearing (b) Meshing in the region of the fault

3 RESULTS & DISCUSSION

The study is performed for faultless bearings, inner race defect bearings, and outer race defect bearings using identical forces, boundary conditions, and parameters.For all the models the mesh size is considered as 1 mm.

The face of the outer ring is assigned a fixed support condition. A constant force of 200N is applied in the z-direction on the inner faces of the inner and outer rings to mimic the radial load that the bearing experiences in normal running conditions. The inner race is given the suitable angular velocity in the y-direction which is to be varied during the analysis.

The analysis is to be carried out for a set time of 0.0001 seconds executing E^{+08} cycles. The output controls are changed to provide information about the solution cycle-wise. The solution is to include the overall stress, the directional deformation of the model, and the total acceleration experienced by the inner and outer rings throughout the analysis.

3.1 Comparison between healthy bearings and bearings with defects

3.1.1 Evaluation of von Mises stresses

A constant velocity of 5000 RPM over an analysis period of 0.0001 seconds is assigned to the inner race in each of the conditions. A constant force of 200 N on the inner and outer races is also assigned in the z-direction. The von Mises stress developed in a body is a direct function of the homogeneity in the geometry of the particular body. Sudden changes in geometry result in the development of stress concentration hence increasing the overall stress developed in the body by a good margin. The bearing with the outer ring defect has the greatest stress developed over time.This is due to a change in geometry of the outer ring in which a cuboidal defect is present resulting in the formation of stress concentration near the defect. Since the outer defect is larger, the stress generated in bearing with the inner defect is smaller.Due to the presence of even geometry, the stress developed in the healthy bearing was found to be least.The stress of an inner defect ring with a maximum stress of 293.95MPA develops with time in Figure 7. The equivalent stress of a bearing with an external ring defect with a maximum stress of 1040.1 MPa is shown in Figure 8. The equivalent stress of a bearing with no defects with stress as high as 728.72 MPa is shown in figure 9.

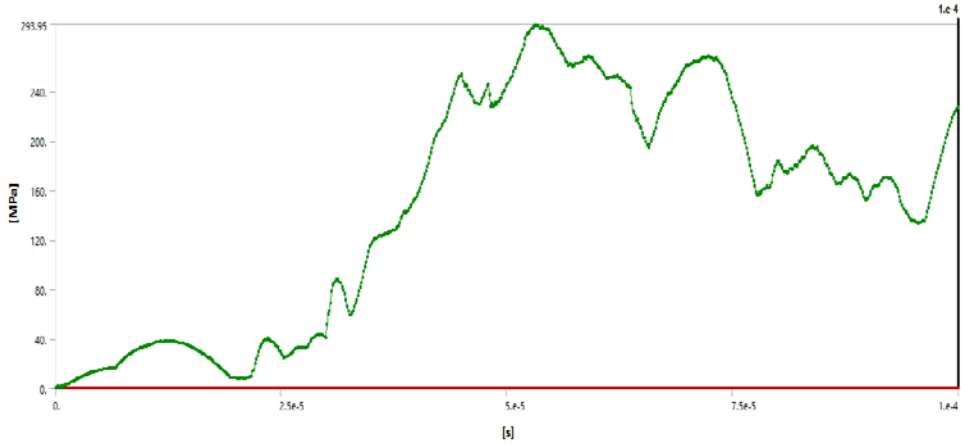

Figure 7: Equivalent stress developed over time for a defective inner ring bearing.

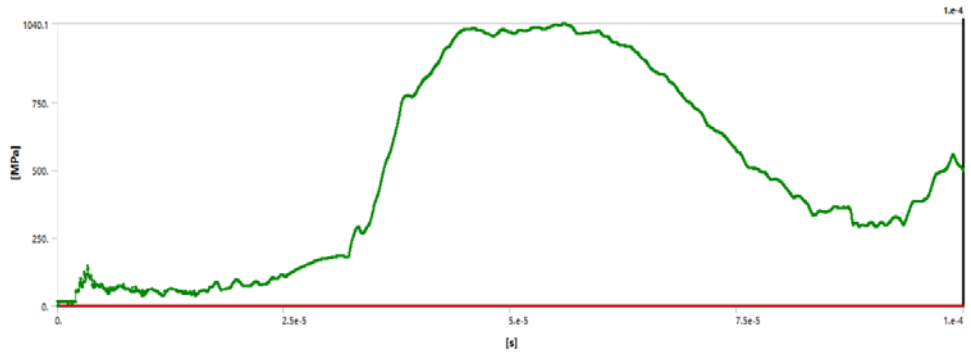

Figure 8: Equivalent stress developed over time for a defective outer ring bearing.

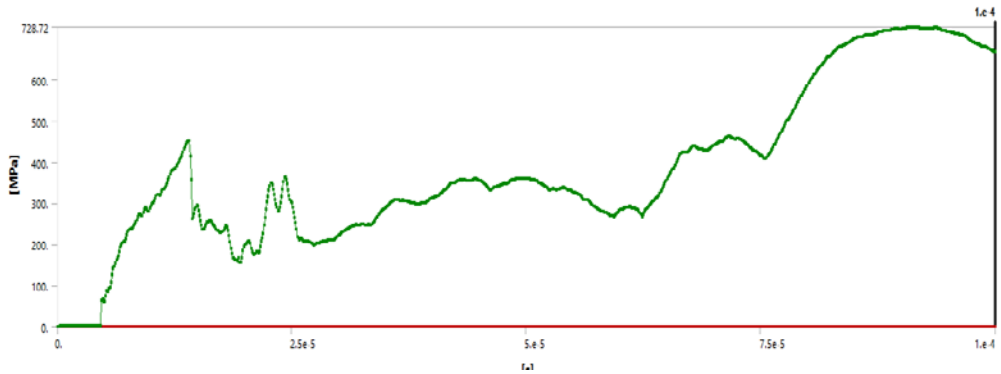

Figure 9: Equivalent stress developed over time for a bearing with no defect.

3.1.2 Directional Deformation

The inner race rotates with the given angular velocity. As a consequence, the highest stress concentration occurs in the balls of both healthy and defective outer rings, and the retainer of defective inner rings.The contact between the rotating inner ring and the balls/retainer with stress concentration results in the higher directional deformation in the inner ring. Since the angular velocity dominates the size of the bearing, the directional deformation generated in the defective inner ring bearing is greater than that produced in the bearing with the outer ring.The direction deformation of a bearing with an inner ring defect, an outer ring defect, and a bearing with no defect is shown in Figure 10.

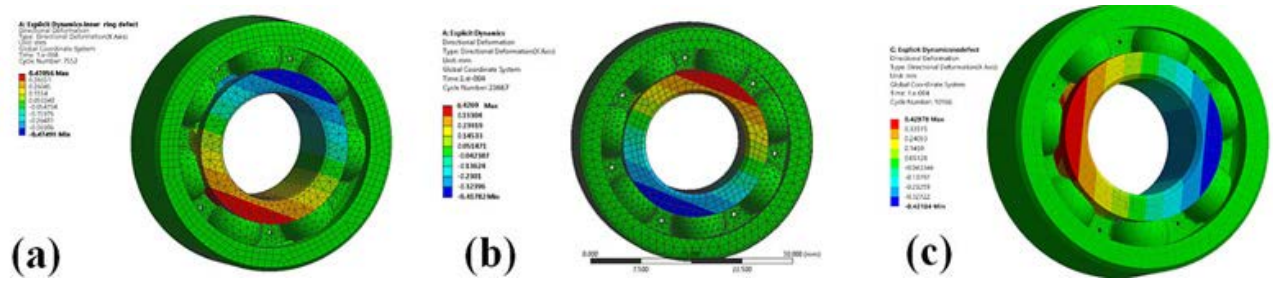

Figure 10: (a) A bearing with an inner ring defect undergoes directional deformation. (b) Directional deformation of a defective outer ring bearing (c) Directional deformation of a non-defective bearing

The deformation pattern was found to be similar for all three types. However, the defective inner ring bearing has a maximum directional deformation of 0.47 mm.

3.1.3 3.1.3 Vibration Signature of inner ring

An acceleration probe is added to the inner ring before analysis. The result obtained is a graph of acceleration of the inner ring vs time for a given RPM. The spikes in the graph indicate the various contacts ensuing and the effect of forces applied. The peak point in the graph indicates the point where the ball falls off/tends to fall into the defect. This point of peak occurs later for the bearing with the defect of the external ring and is larger.The contact between the rotating inner race and the balls and retainer is shown by the highest point in the graph of the healthy bearing.Figure 11 depicts the Vibration signature of a defective inner ring bearing. Figure 12 depicts the vibration signature of a defective outer ring bearing. Figure 13 depicts the vibration signature of a non-defective bearing.

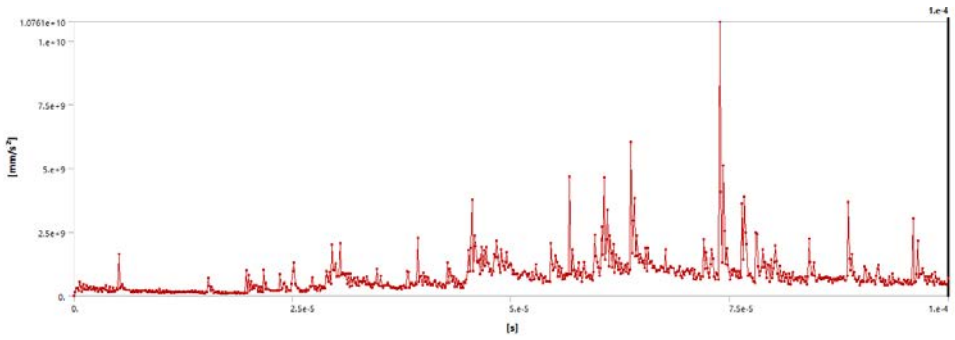

Figure 11: The vibration signature of a bearing with a defective inner ring

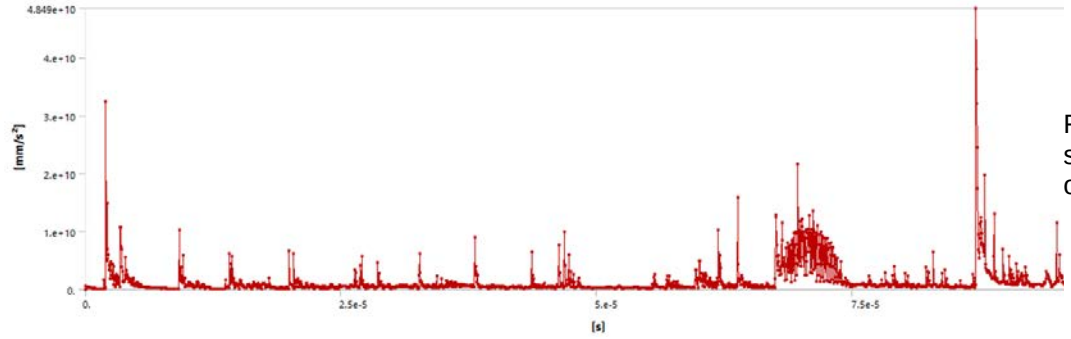

Figure 12: Vibration signature of a defective outer ring bearing

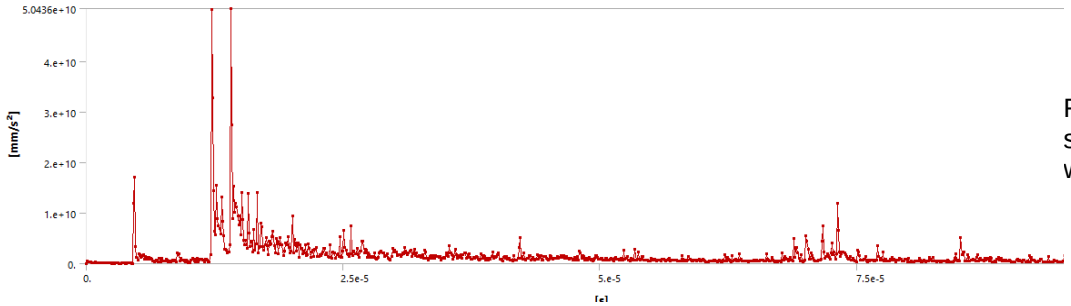

Figure 13: Vibration signature of a bearing with no defect

The peak point on the bearing with interior defect graph represents the moment at which the ball falls off/tends to fall into the defect, generating vibration in the inner race that is progressively transferred to the outer race, resulting in a sharp increase in value over time. This peak point occurs sooner for the bearing with the external ring defect and is of more size because as the inner ring begins to rotate, the ball falls into the external race that has a larger defect. The peak point in the graph of the healthy bearing indicates that contact between the rotating inner race and the balls and retainer has taken place and the succeeding vibration effects have been transferred to the outer race.

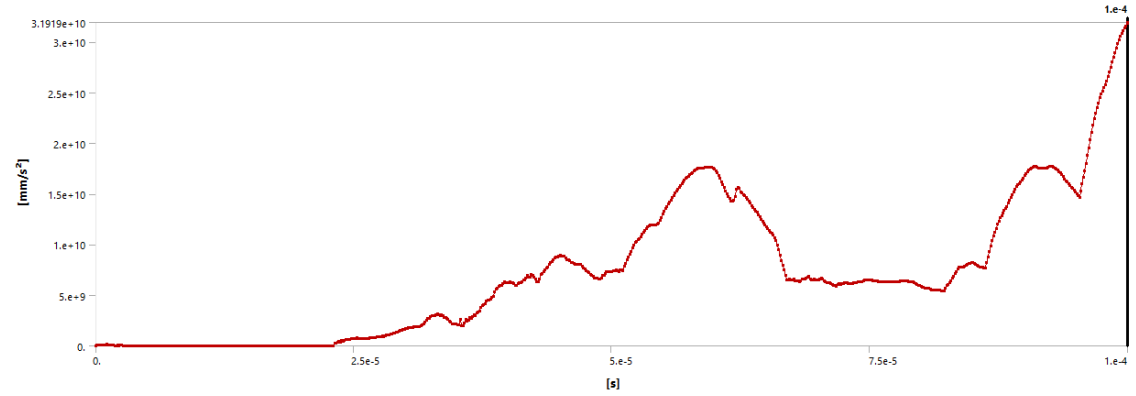

Figure 14: The vibration signature of a bearing with a defective inner ring

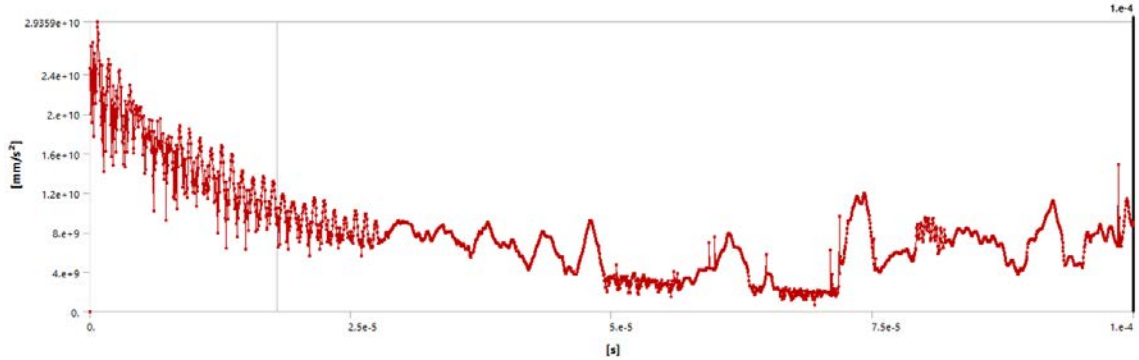

Figure 15: Vibration signature of a defective outer ring bearing

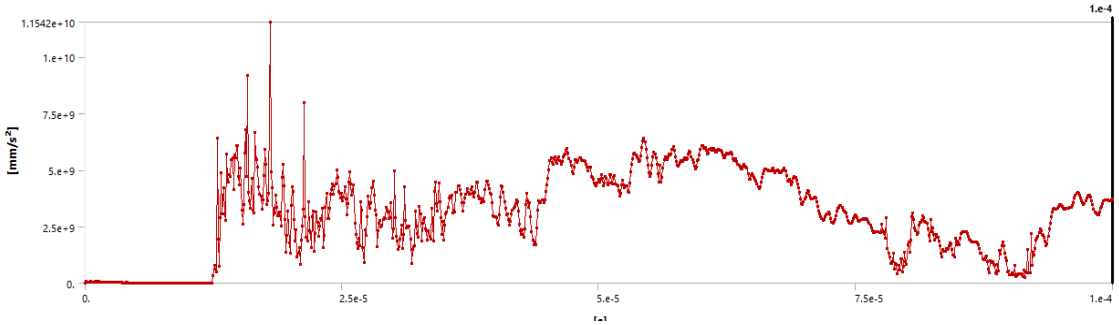

Figure 16: Vibration signature of a bearing with no defect

Table 3 shows the results obtained at 5000rpm for inner and outer defects on bearings and healthy bearings.

Table 3: Different parameters analyzed at 5000 RPM for defect and healthy bearing

Parameters	Inner Ring Defect	Outer Ring Defect	Nodefect
Equivalent Stress (MPa)	226.89	498.92	669.71
Directional Deformation (mm)	0.47056	0.4269	0.42978
Inner Ring:			
TotalAcceleration(mm/s^2)	4.084e^{+09}	4.9851e^{+09}	3.9016e^{+08}
MaximumAcceleration over time(mm/s^2)	1.0761e^{+10}	4.849e^{+10}	5.0436e^{+10}
OuterRing:			
TotalAcceleration(mm/s^2)	3.1919e^{+10}	9.0301e^{+09}	3.7036e^{+09}
MaximumAcceleration over time(mm/s^2)	3.1919e^{+10}	2.9359e^{+10}	1.1542e^{+10}

3.2 Limitations of the current study

In the current work, a healthy bearing is analyzed along with the artificially defected generated bearing. Estimation of the amplitude of vibrations is carried out at 5000 RPM, a load of 200 N, and at different deformity sizes, 3 mm and 4 mm on bearing races are carried out. However, in real conditions, these deformity sizes vary. So, it is required to consider the different deformity sizes to know the effect of this deformity. In the current work a constant 5000 RPM, a load of 200 N is used. But angular velocity with different RPM and load can be considered along with variation in the deformity sizes to estimate the life of the bearing surface with change in these parameters.

4 CONCLUSION

The uniformity of the geometry has a bearing on stress concentration developed in the part. A sudden change in geometry would subsequently spike the stress values. The stress developed over time in a faulty bearing is, therefore, more than that in a healthy bearing due to the presence of the cuboidal hole in the bearing race. The dimension of the defective outer race is larger than the defective inner race leading to a greater value of stress concentration at this point leading to the development of greater stress in the former case. The inner race rotates with the given angular velocity while the outer race remains stationary. As a result, the greatest stress concentration is developed in the balls of healthy bearings and the outer rings of bearings with outer ring defects, and in the retainer of bearings with inner rings defects, as a result of the initial interaction of the inner race with the balls/retainer when the bearing starts rotating instantly.The contact between the rotating inner ring and the balls/retainer with stress concentration results in the greatest directional deformation being produced in the inner ring. As an exception, the directional deformation produced in the defective inner ring bearing is more than that of the outer ring because angular velocity dominates the size of the bearing. The values of stress developed, directional deformation and vibrational signatures for the inner and outer race are markedly greater for the defective outer race bearings than the defective inner race bearings. In the current work a constant 5000 RPM, a load of 200 N is used. But angular velocity with different RPM and load can be considered along with variation in the deformity sizes to estimate the life of the bearing surface with change in these parameters.

5 ACKNOWLEDGMENTS

The authors would like to express their gratitude to the Department of Aeronautical and Automobile Engineering at Manipal Institute of Technology, Manipal Academy, Manipal for supporting with the necessary computing resources for this research.

6 REFERENCES

[1] Z. Yongqi, T. Qingchang, Z. Kuo, L. Jiangang, Analysis of Stress and Strain of the Rolling Bearing by FEA method, Phys. Procedia. 24 (2012) 19–24. doi:10.1016/j.phpro.2012.02.004.

[2] V.R. Bajaj, M.E.C.A.D.C.A.M. Student, Finite Element Analysis of Integral Shaft Bearing, 3 (2015) 28–36.

[3] S.C. Sharma, V. Kumar, S.C. Jain, R. Sinhasan, M. Subramanian, Study of slot-entry hydrostatic/hybrid journal bearing using the finite element method, Tribol. Int. 32 (1999) 185–196. doi:10.1016/S0301-679X(99)00032-8.

[4] N. Tandon, A. Choudhury, Review of vibration and acoustic measurement methods for the detection of defects in rolling element bearings, Tribol. Int. 32 (1999) 469–480. doi:10.1016/S0301-679X(99)00077-8.

[5] E. Claesson, Modelling of roller bearings in ABAQUS Master ' s Thesis in the Applied Mechanics, (2014).

[6] A. Utpat, Vibration Signature analysis of defective deep groove ball bearings by Numerical and Experimental approach, Int. J. Sci. Eng. Res. 4 (2013) 592–598.

[7] M. Motooka, A finite element method used for contact analysis of rolling bearings, (2015).

[8] Y.G. Wei, Y.K. Liu, Finite element analysis of the roller bearing used in rolling mill, Appl. Mech. Mater. 367 (2013) 141–144. doi:10.4028/www.scientific.net/AMM.367.141.

[9] A. Nabhan, Contact Stressdistribution of Deep Groove Ball Bearing Using Abaqus, J. Egypt. Soc. Tribol. 12 (2015) 49–61. doi:10.21608/JEST.2015.79986.

[10] J. Xu, J. Zhang, Z. Huang, L. Wang, Calculation and finite element analysis of the temperature field for high-speed rail bearing based on vibrational characteristics, J. Vibroengineering. 17 (2015) 720–732.

[11] M. Amarnath, R. Shrinidhi, a Ramachandra, S.B. Kandagal, Prediction of Defects in Antifriction Bearings using Vibration Signal Analysis, Time. (2004) 88–92.

[12] T. Gopalakrishnan, R. Murugesan, Contact Analysis of Roller Bearing Contact Analysis of Roller Bearing Using Finite Element, Vels J. Mech. Eng. 2 (2015) 1–5.

[13] D. Azad, K. Ramji, T.N. Officer, Identification of bearing assembly defects using Finite Element Analysis and Condition Monitoring Techniques, 1 (2012) 1–13.

[14] B. Deng, Y. Guo, A. Zhang, S. Tang, Finite element analysis of thrust angle contact ball slewing bearing, IOP Conf. Ser. Mater. Sci. Eng. 274 (2017). doi:10.1088/1757-899X/274/1/012096.

[15] Y. Shao, W. Tu, F. Gu, A simulation study of defects in a rolling element bearing using FEA, ICCAS 2010 - Int. Conf. Control. Autom. Syst. (2010) 596–599. doi:10.1109/iccas.2010.5669813.

[16] H. Saruhan, S. Saridemir, A. Çiçek, I. Uygur, Vibration analysis of rolling element bearings defects, J. Appl. Res. Technol. 12 (2014) 384–395. doi:10.1016/S1665-6423(14)71620-7.

[17] A.T. Ravindra, K.K. Nilesh, M. P.Shyam, Vibration analysis of ball bearing, Int. J. Sci. Res. 4 (2015) 2655–2665. https://www.ijsr.net/archive/v4i5/SUB154835.pdf.

[18] S.R. D, P.S.S. Kulkarni, Vibration Analysis of deep groove ball bearing using Finite Element Analysis, 5 (2015) 44–50.

[19] SKF 6202 Deep groove ball bearings, (2021) 3–6.

[20] S. Tyagi, S.K. Panigrahi, Transient Analysis of Ball Bearing Fault Simulation using Finite Element Method, J. Inst. Eng. Ser. C. 95 (2014) 309–318. doi:10.1007/s40032-014-0129-x.

[21] H. Huang, Z. Yuan, W. Kang, Z. Xue, X. Chen, C. Yang, Y. Ye, J. Leng, Study of the sealing performance of tubing adapters in gas-tight deep-sea water sampler, Int. J. Nav. Archit. Ocean Eng. 6 (2014) 749–761. doi:10.2478/IJNAOE-2013-0212.

[22] M.B. Davanageri, S. Narendranath, R. Kadoli, Finite Element Wear Behaviour Modeling of Super duplex stainless steel AISI 2507 Using Ansys, IOP Conf. Ser. Mater. Sci. Eng. 376 (2018). doi:10.1088/1757-899X/376/1/012131.

[23] L. Gardner, The use of stainless steel in structures, Prog. Struct. Eng. Mater. 7 (2005) 45–55. doi:10.1002/pse.190.

Paper submitted: 13.09.2021.

Paper accepted: 25.12.2022.